

Short Note

Performance Test of a Commercial Rotational Motions Sensor

by Joachim Wassermann, Susanne Lehndorfer, Heiner Igel, and Ulrich Schreiber

Abstract The application of rotational motion sensors has only recently proven to give new ways of measuring seismic-wave-field properties when comparing the recorded data with seismograms of collocated traditional seismometers. The data in these test cases were produced using either sophisticated and thus expensive ring laser technology or cumbersome seismic array techniques including some restrictive assumption about the wave field. In this article, we want to test the performance of one of the first medium-priced commercial rotational motion sensor (eentec *R1*) by comparing its output with the aforementioned classical array-derived rotational motions. The data set consists of seismic array and rotational motion measurements that were performed during a demolition blast of a 50 m high building in the city of Munich (Germany). In addition to the simple comparison of the outputs, we want to classify the performance of the two methods by comparing derived wave-field properties with the result of classical frequency-wavenumber (f - k) array analysis. The results of this experiment demonstrate that, when using an array technique for estimating rotational motions, much effort in site selection, array design, and *a priori* knowledge of subsurface conditions is needed. It also becomes evident that the performance of an array and its estimated quantities strongly depends on the number of deployed seismic stations. Given the uncertainties in both the array-derived measurements and the rotation sensor transfer function, it is difficult to quantify the accuracy of the rotation sensor data, which indicates the need for further extensive laboratory and field testing.

Online Material: Digital seismograms with metadata for the demolition blast.

Introduction

Following the statement of Aki and Richards (2002) that a complete representation of the Earth's ground motion needs next-to-translational motions along with the recording of rotations and strain, several articles demonstrate that it is possible to compute rotational motions in the far field of a seismic source using small aperture seismic arrays and derived spatial derivatives, respectively (Spudich *et al.*, 1995; Suryanto *et al.*, 2006; Langston, 2007; Spudich and Fletcher, 2008). Testing a geodetic ring laser for its sensitivity to rotational motions, Suryanto *et al.* (2006) showed that this ring laser demonstrates equal or even superior performance in comparison to the vertical component of array-derived rotational motions. The authors conclude that noise in the computed array-derived rotational motions is strongly dependent on the number of stations used. Igel *et al.* (2005, 2007) demonstrate that using the ratio of transverse acceleration of a traditional three-component translation sensor (i.e., a seismometer) and rotational motions could lead to new techniques for measuring the apparent wave velocity and back

azimuth without the need for deploying a complete seismic array.

An additional motivation for designing new rotational motion instruments originates from the inherent restrictions of array-derived rotation motions. Strictly speaking, its formal derivation is only valid assuming a linear gradient of the wave field, that is, mainly in its far field and without further pollution of the seismometers by tilt signals (assumptions that may not always be fulfilled in the real world). In light of the increasing interest in measuring rotational motions, particularly in connection with earthquake engineering and strong ground-motion problems, it is important to thoroughly investigate the performance of rotation sensors, particularly those that can be deployed in the field. Here we report on a field test of the eentec *R1* three-component rotation sensor and estimate its performance by comparing it with rotational motions derived from a seismic array as well as classical seismic array analysis. Seismic energy was generated by a collapsing building initiated by explosions.

Experiment Setup and Discussion

The data used in this study consist of a seismic seven-element array with an aperture of 70 m and mean station distance of 20 m (Fig. 1). In the center of the array, an eentec R1 rotational motion sensor is collocated to a Streckeisen STS-2 broadband sensor (see Fig. 1, station 01) forming the core elements of the experiment. The sampling rate is set to 200 Hz for all used instruments. The distance from the eentec R1 location (station 01), the reference point of the array, to the blast site (the black square in Fig. 1) is approximately 250 m with a back azimuth of 280° . The building and the array are both situated on a uniform thick layer of glacial rubble, which makes differences in site amplification of array stations rather unrealistic. The blast itself consists of 150 kg explosives sequentially fired to reduce ground shaking. It was hoped, however, that the blasted building could produce a high portion of rotational motions and tilt, as it was going to fulfill a twisted motion while collapsing. \oplus The seismograms and rotational seismograms of the demolition blast can be found in the electronic edition of *BSSA*.

Following Spudich and Fletcher (2008), we first compute the frequency band for which the error of the array-derived rotational motion remains below 10%. The error is caused by deviations from the assumed linear gradient of the

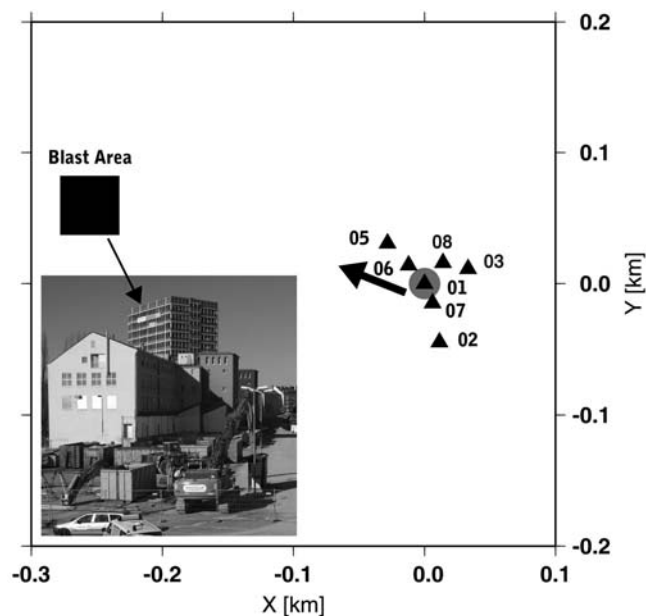


Figure 1. The seismic array setup that was used in this study is featured; the relative location of the demolition blast is indicated by a square. The locations of the seismometers are indicated by black triangles. At station 01, a Streckeisen STS-2 broadband seismometer is collocated with the eentec R1 sensor (gray circle). 02, 03 are additional sites of STS-2 broadband seismometers; 04–08 mark the location of short-period (1 Hz) sensors. The inset gives an impression about the size of the building and the distance towards the array, respectively. The black arrow indicates the viewing direction of the photo. Photo courtesy of S. Egdorf.

wave field and strongly depends on the aperture of the array. As a first approximation, we assume a wave speed of 1000 m/sec as an initial guess. Using the aperture of 70 m, which was also chosen to apply the classical frequency-wavenumber (f - k) array analysis, we estimate the upper corner frequency to be at 3.5 Hz. Reducing the array's aperture to 35 m by reducing the number of stations will therefore result in a corner frequency of 7 Hz. In this context, it is important to note that the main seismic energy during the blast and subsequent collapse was radiated in a narrow frequency band around 6 Hz.

The lower frequency limit was chosen because of mixing broadband (Streckeisen STS-2 at 01, 02, and 03) and short-period (1 Hz; MarkL4/3C at stations 05, 06 and Lenartz Le3Dlite at stations 07, 08) seismometers in the experiment. Although all of the seismograms are corrected for the instrument transfer function down to 0.5 Hz before computing spatial derivatives, the frequency limit was set to 1 and 0.8 Hz, respectively, in order to further suppress possible phase shifts caused by erroneous transfer functions. It can be shown that uncertainties in the transfer function have a strong influence, especially in the vicinity of the corner (eigen) frequency of an instrument. This may cause problems in the rotational motion seismograms, which we will discuss later in more detail. In Figure 2, data records of all directly comparable measurements (transverse acceleration, rotational motions, and array-derived rotations in their vertical component) are shown following the initial blast in two different frequency bands. In order to evaluate the influence of the bandwidth and the number of used stations for the following comparison between different sensors and sensor configurations, we filter the data with a zero phase band pass between 0.8–5 Hz and 1–8 Hz, respectively. While the first band pass (Fig. 2a–d) is at least near the optimum frequency versus aperture relationship given by Spudich and Fletcher (2008), the second band pass (Fig. 2e–h) includes the main energy peak of the radiated frequencies. It becomes immediately apparent that the eentec R1 sensors have a larger amount of noise present in the lower frequency range. Additionally, the reduced similarity between the array-derived rotational motions and the transverse acceleration in the 0.8–5 Hz frequency band, in comparison with the corresponding traces for the 1–8 Hz case, is remarkable. The lower performance is visible even when only four stations are used. This may reflect problems in computing array-derived rotational motions when a significant portion of the recorded signal contains uncorrelated noise.

The next step is to compare array-derived rotational motions, computed using the method proposed by Spudich *et al.* (1995) with signals recorded by the R1 sensor. Following aforesaid statement, we perform this analysis in the frequency band between 1 and 8 Hz but using different array sizes. We do this even though we may violate the estimation made by Spudich and Fletcher (2008) (at least at some points). The comparison itself shows a surprisingly good agreement (Figs. 3, 4, and 5) with the case of rotational sig-

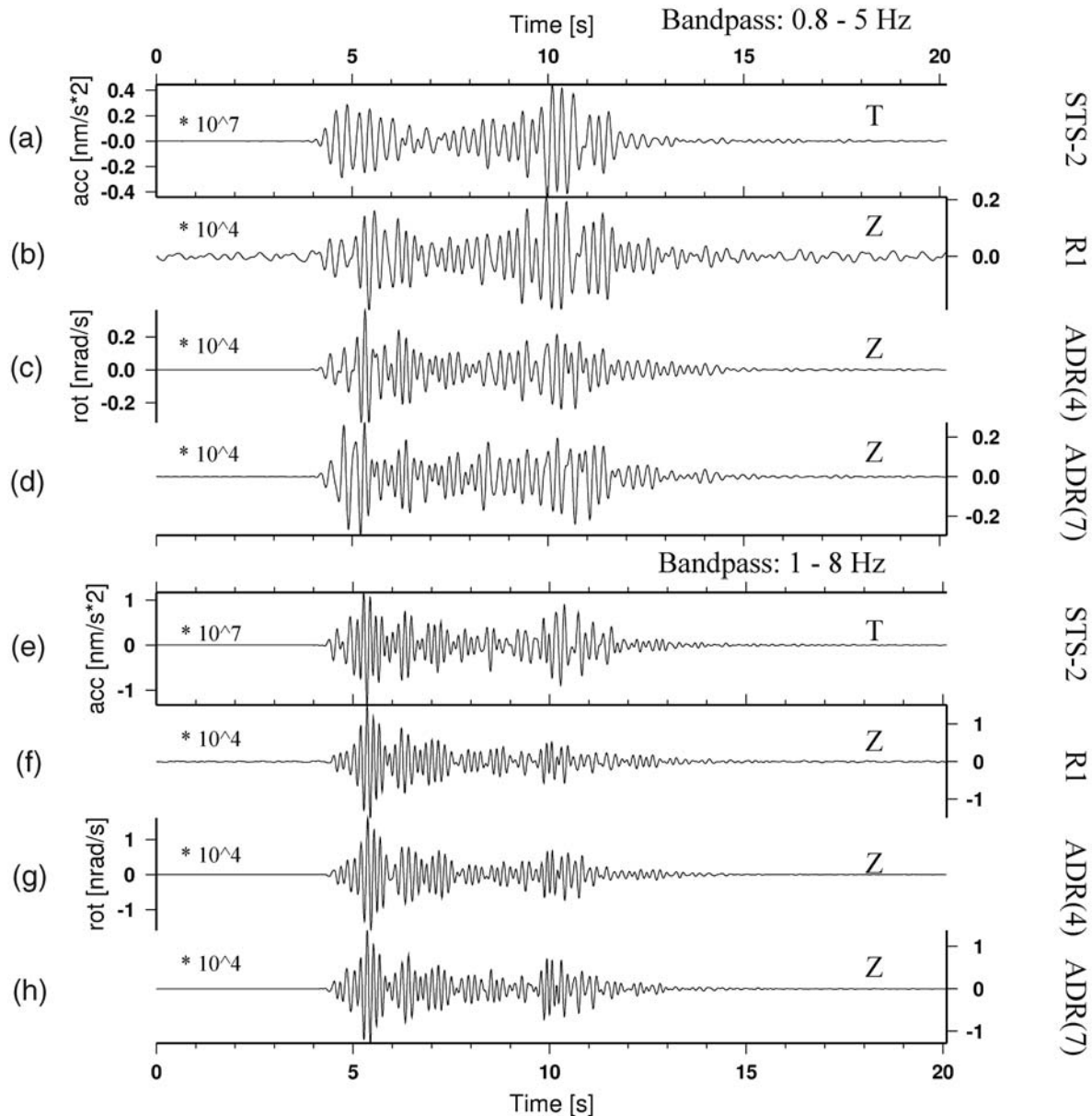


Figure 2. Estimated transverse acceleration, using station 01 (STS-2) and the building's back azimuth, R1. Vertical component output and array-derived rotations using a four- (01, 03, 07, and 08) and seven- (01, 02, 03, 05, 06, 07, and 08) element array in different frequency bands are shown. (a)–(d) represent the recorded signals in a band pass of 0.8–5 Hz, while (e)–(h) show the same quantities but in a frequency band 1–8 Hz, including the dominant frequency at 6 Hz.

nals around vertical (Z) and northern (N) axes in most of the cases. Why this good match in the waveforms cannot be seen in the eastern (E) components is still unclear (see Fig. 5 for the seven-element array). If scattering is the main source of error for this component (E component corresponds to twisting motion that is perpendicular to the source receiver axis; see Fig. 1), it is still unclear why the rotational motion sensor is more sensitive to this scattering wave than the array stations. It is possible that the array assumption of the correlated signals is violated; therefore, these scattered waves are suppressed. Figures 3, 4, and 5 also confirm the statement of Suryanto *et al.* (2006) that the number of used stations for

computing spatial derivatives significantly changes the result. The amplitudes especially change dramatically when increasing the number of array elements. Assuming a correct gain of the eentec R1 sensor, the seven-element array shows a nearly perfect fit in amplitude (Fig. 5), while the five-element array overestimates the rotational motion amplitudes by a factor of 30% (Fig. 4).

When focusing on details, differences between R1 and array-derived rotation become apparent. The array-derived rotational motions show a significant phase shift, especially in its N component compared to the R1 signals (Figs. 3, 4, and 5). Phase shifts are present for the four-, five-, and seven-

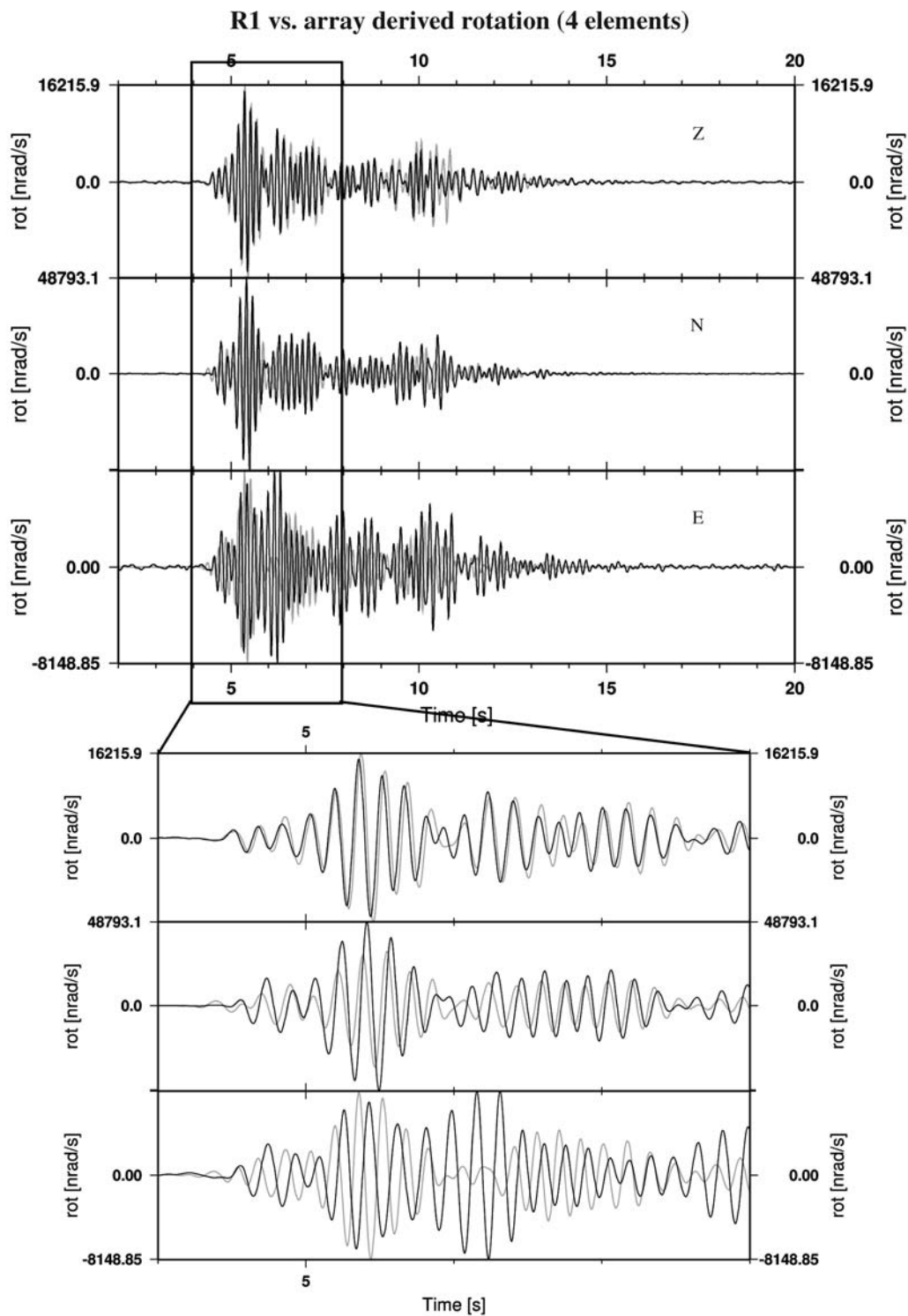


Figure 3. Direct comparison between *R1* (black line) and a four-element array (01, 03, 07, and 08; see Fig. 1) derived rotational motion (gray line) in all components. A pronounced mismatch in the amplitude and phase is visible.

sensor array, respectively, but seem to be more pronounced for the four- and seven-sensor array (Figs. 3 and 5). Even worse, the phase shift is not constant during the complete recording. Possible reasons for the phase misalignment could be the always present noise, the problems with the sensor calibrations, or both. The first seems to be reasonable, as the

recording site was within a city with heavy traffic in its direct vicinity. However, even as the instrument correction procedure that was applied to the raw data should reduce possible influences of erroneous transfer functions, phase shifts as possible causes of not precisely calibrated sensors are a well-known problem. Because phase and amplitude

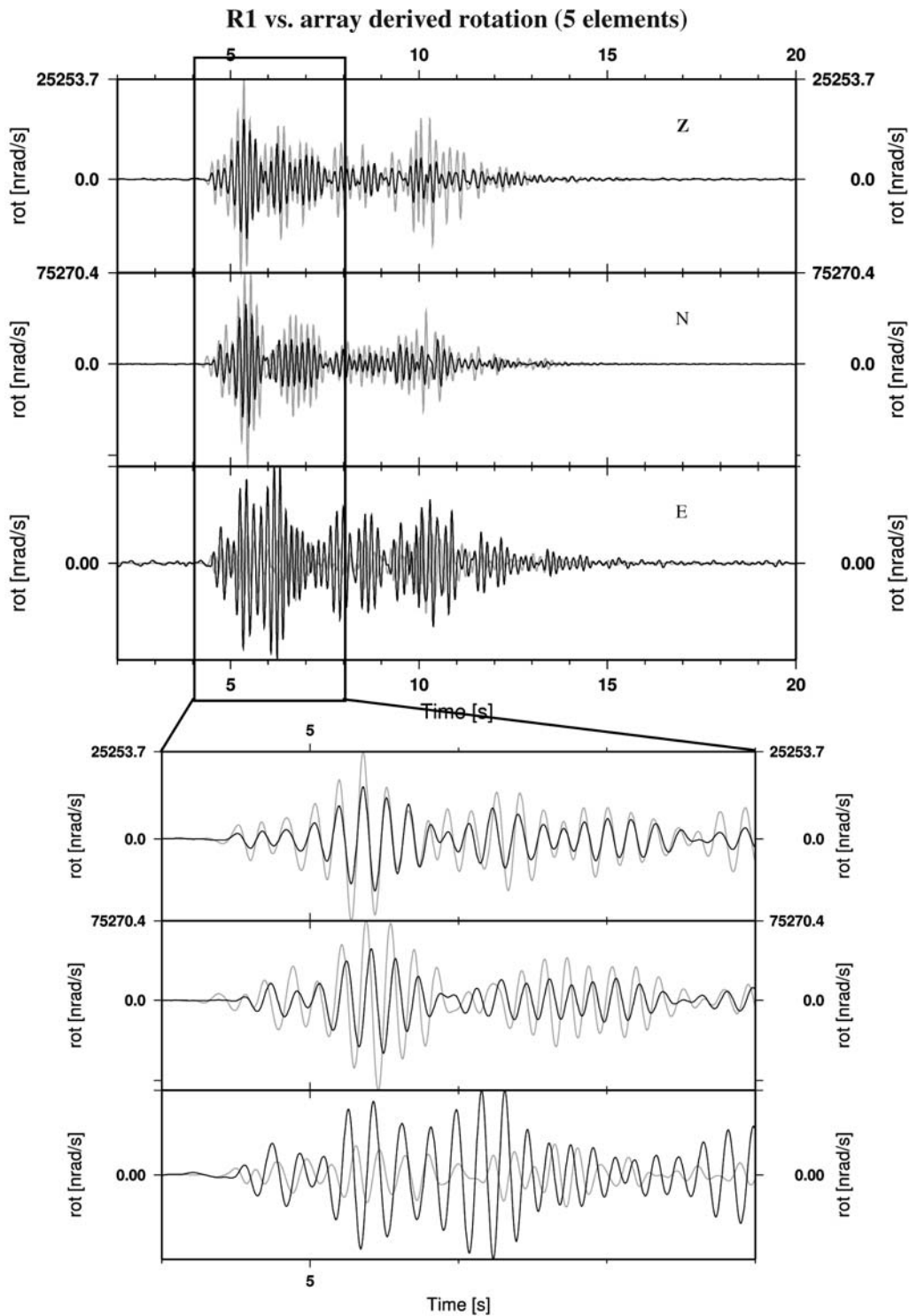


Figure 4. Same as in Figure 3 but comparing $R1$ (black line) and five-element array (01, 02, 03, 07, and 08; see Fig. 1) output (gray line). While the amplitude still deviates, the phase match is nearly perfect in the Z component.

mismatch shifts are worse using the four-element array, which is more or less consistent with lower error rates according to Spudich and Fletcher (2008), as well as the seven-element array, which includes two older seismometers of the same type (Mark L43C 1 Hz), we restrict our further analysis to the comparison with the five-element array data. This may

lead to incorrect velocity estimations (Igel *et al.*, 2005, 2007) but should at least give stable results.

The performance tests presented so far were done by comparing two different ways of measuring rotational motions for which the errors are only partially known. On one hand, the transfer function of the eentec $R1$ sensor, its tem-

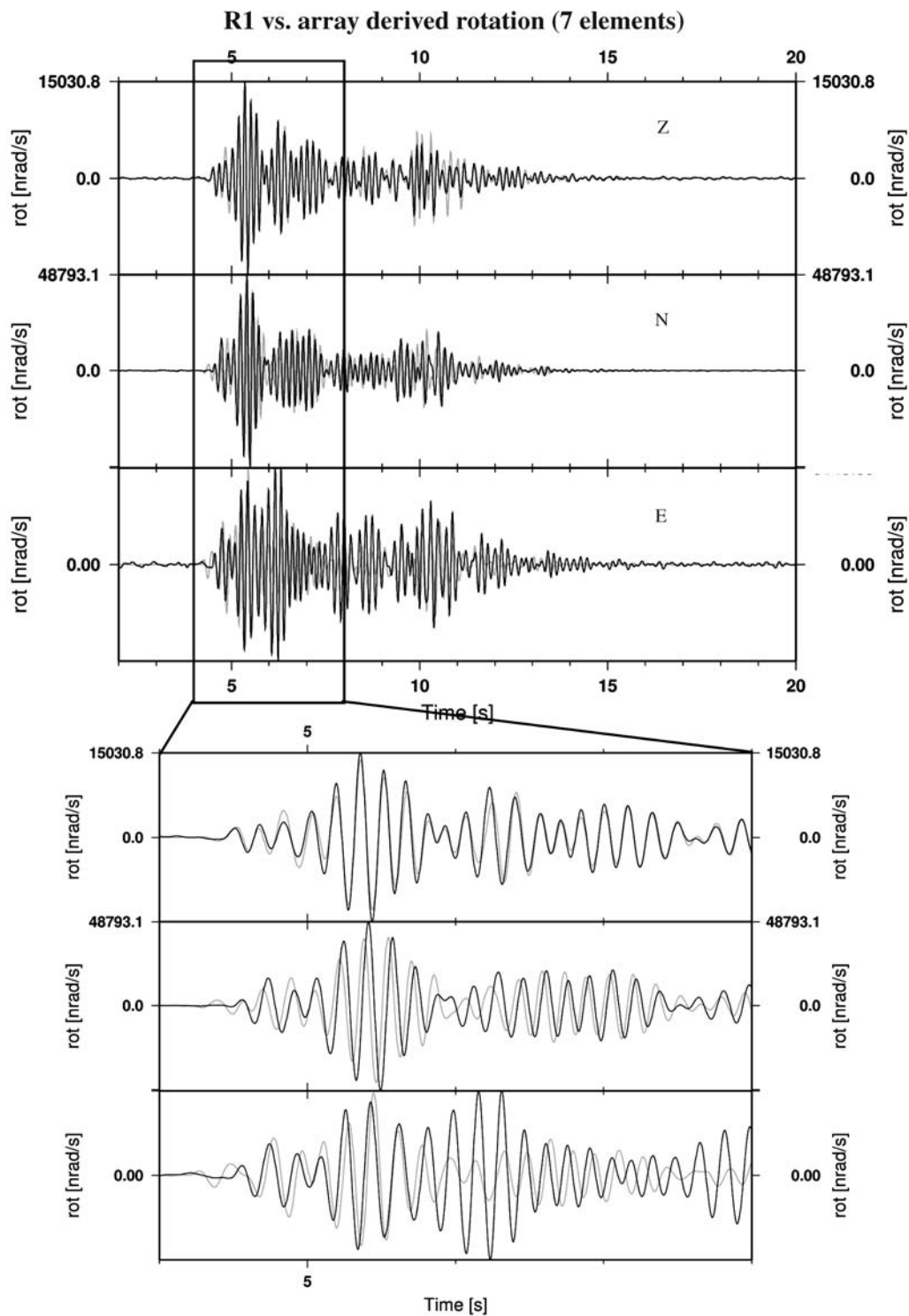


Figure 5. Same as in Figure 3 but comparing $R1$ (black line) and seven-element array (01, 02, 03, 05, 06, 07, and 08) output (gray line). While the amplitude now fits perfectly, the phase mismatch is increasing.

poral stability, cross talk between components, and possible influence of translational motion on the sensors is still a matter of debate. On the other hand, assumptions needed to justify array-derived rotational motion, that is, uniform spatial gradient, size of the array versus curvature of the gradient (Spudich and Fletcher, 2008), and tilt- (rotational-) free re-

cordings of translational motions may not be fulfilled in real world applications.

In order to test the overall quality of the two ways to measure rotational motions, we compare the results of standard f - k seismic array techniques: apparent velocity, back azimuth, semblance (see, e.g., Kvaerna and Ringdahl, 1986)

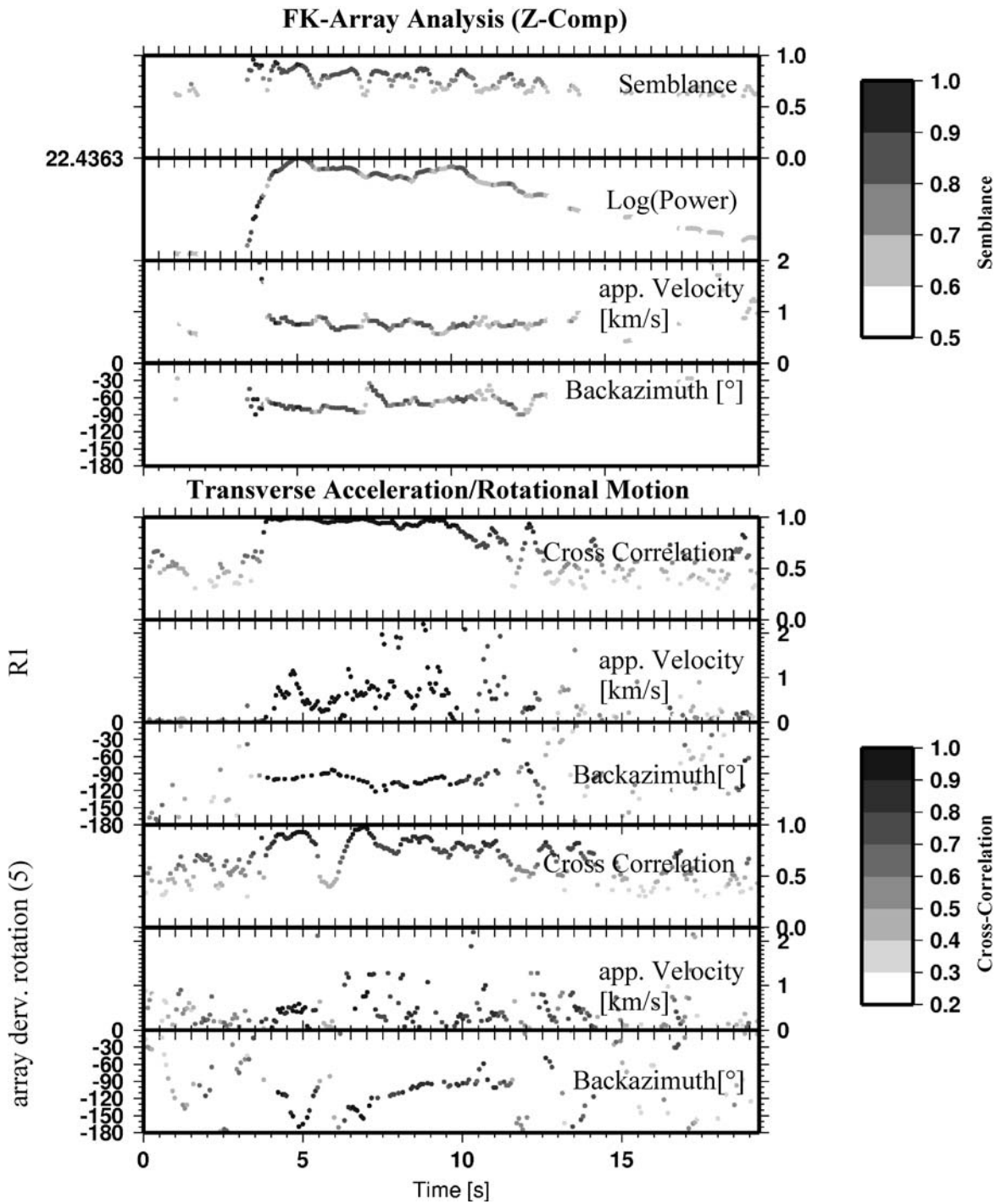


Figure 6. Comparison between standard f - k array analysis output and parameters computed using rotational motions recordings. Semblance, logarithmic beam power, apparent velocity, and back azimuth are shown using a 0.68 sec sliding window in a frequency band between 1 and 8 Hz. Only values with a semblance larger than 0.6 are shown. The maximum of the cross-correlation coefficient computed in a 0.68 sec sliding window between the Z component of the R1 sensor and the transverse acceleration (T axis) of the collocated seismometer, the apparent velocity estimated by the ratio between acceleration, and rotational motions and the back azimuth are shown. All estimates are computed while probing the optimal rotation of the horizontal seismometer components with respect to maximization of the cross-correlation coefficient with a time lag at zero.

with the parameter computed following the procedure of Igel *et al.* (2005, 2007): maximum cross correlation in a sliding window of rotational motions with transverse acceleration, back-azimuth value depending on the maximum cross correlation when probing the correlation for different azimuth values, and the apparent velocity computed by the ratio of transverse acceleration (with respect to maximizing the cross correlation) versus rotational motions (Fig. 6).

Even as the array to source distance is within just several wavelengths at 6 Hz and the assumption of plane wave incidence may not be fully correct, Figure 6 clearly shows the advantage of using classical seismic array techniques: the suppression of incoherent noise. While variations in time of the maximum of cross-correlation coefficients and semblance look quite similar, the results for apparent velocity and back azimuth strongly deviate for both *R1* and array-derived rotations. Deviations in the apparent velocities can be quite naturally explained up to some degree by the different sensitivity of the methods to different wave types, that is, Rayleigh waves in the case of *f-k* analysis and Love waves in the case of transverse acceleration versus rotational motion ratio. However, the large deviations in the back azimuth must be explained differently. Again, noise may play an important role in erroneous estimation. Another possible reason is a misorientation of the translation sensor. A misalignment of more than 30°, however, as seen in Figure 6 for both methods, seems unreasonable.

In summary, the eentec *R1* sensor seems to give reasonable results for at least the higher frequency portions of the analyzed signals. The experiment clearly shows problems and difficulties when using seismic arrays for recording rotational motions. Next to differences in site responses, noise seems to play a dominant role in the quality of the estimations. A larger number of sensors will suppress present noise and will therefore increase the reliability of the measurement even though the assumption of a uniform gradient may be violated.

On the other hand, some doubt remains about the quality of the calibration of the eentec *R1* sensor, especially in the lower (<1 Hz) frequency range. Therefore, the sensor should undergo more careful long-term tests regarding stability and contamination by translational motions. A possible new application, which combines advantages of both techniques, would be to collocate a seismic array with the same number of rotational sensors in order to reduce noise effects on the different sensor types.

Data and Resources

All data used in this study were provided by the Geophysics Section and the Geophysical Observatory of the Ludwig–Maximilians University Munich. The measurements were performed using equipment of the Geophysical Observatory and the Seismological Central Observatory Graefenberg (BGR).

Acknowledgments

We are grateful to H. Blachnitzky for allowing us to measure the blast in its near field. Comments and corrections made by P. Spudich significantly improved the manuscript and are greatly appreciated. Furthermore, we would like to express our thanks to S. Egdorf and W. Bauer for their technical support and assistance even on short notice. Many thanks also to E. Wetzig from the Graefenberg Array (BGR) for borrowing two of the deployed broadband sensors.

References

- Aki, K., and P. G. Richards (2002). *Quantitative Seismology*, Second Ed., University Science Books, Sausalito, California.
- Igel, H., U. Schreiber, A. Flaws, B. Schuberth, A. Velikoseltsev, and A. Cochard (2005). Rotational motions induced by the *M* 8.1 Tokachi-oki earthquake, September 25, 2003, *Geophys. Res. Lett.* **32**, L08309, doi 10.1029/2004GL022336.
- Igel, H., A. Cochard, J. Wassermann, A. Flaws, U. Schreiber, A. Velikoseltsev, and N. Pham Dinh (2007). Broad-band observations of earthquake-induced rotational ground motions, *Geophys. J. Int.* **168**, no. 1, 182–197, doi 10.1111/j.1365-246X.2006.03146.x.
- Kvaerna, T., and F. Ringdahl (1986). Stability of various *f-k* estimation techniques, NORwegian Seismic ARray (NORSAR) Scientific Report No. 1-86/87, Semiannual Technical Summary, 1 October 1985–31 March 1986, 29–40.
- Langston, C. A. (2007). Spatial gradient analysis for linear seismic arrays, *Bull. Seismol. Soc. Am.* **97**, no. 1B, 265–280, doi 10.1785/0120060100.
- Spudich, P., and J. B. Fletcher (2008). Observation and prediction of dynamic ground strains, tilts, and torsions caused by the *M_w* 6.0 2004 Parkfield, California, earthquake and aftershocks, derived from UPSAR array observations, *Bull. Seismol. Soc. Am.* **98**, no. 4, 1898–1914, doi 10.1785/0120070157.
- Spudich, P., L. K. Steck, M. Hellweg, J. B. Fletcher, and L. M. Baker (1995). Transient stresses at Parkfield, California, produced by the *M* 7.4 Landers earthquake of June 28, 1992: observations from the UPSAR dense seismograph array, *J. Geophys. Res.* **100**, no. B1, 675–690.
- Suryanto, W., J. Wassermann, H. Igel, A. Cochard, D. Vollmer, F. Scherbaum, A. Velikoseltsev, and U. Schreiber (2006). First comparison of seismic array-derived rotations with direct ring laser measurements of rotational ground motion, *Bull. Seismol. Soc. Am.* **96**, no. 6, 2059–2071, doi 10.1785/0120060004.

Department of Earth and Environmental Sciences
Ludwig–Maximilians Universitaet Muenchen
Theresienstrasse 41
D-80333 Munich, Germany
jowa@geophysik.uni-muenchen.de
(J.W., S.L., H.I.)

Forschungseinrichtung Satellitengeodäsie
Technische Universitaet Muenchen
Fundamentalstation Wettzell
Sackenriederstrasse 25
D-93444 Kötzing, Germany
(U.S.)